

# Anisotropic Tensor Renormalization Group

Daiki Adachi<sup>1</sup>, Tsuyoshi Okubo<sup>1</sup>, and Synge Todo<sup>1,2</sup>

<sup>1</sup>*Department of Physics, University of Tokyo, Tokyo, 113-0033, Japan*

<sup>2</sup>*Institute for Solid State Physics, University of Tokyo, Kashiwa, 277-8581, Japan*

We propose a new tensor renormalization group algorithm, Anisotropic Tensor Renormalization Group (ATRG), for lattice models in arbitrary dimensions. The proposed method shares the same versatility with the Higher-Order Tensor Renormalization Group (HOTRG) algorithm, *i.e.*, it preserves the lattice topology after the renormalization. In comparison with HOTRG, our method dramatically reduces the computation cost especially in higher dimensions by renormalizing tensors in an anisotropic way after the singular value decomposition. We demonstrate the ability of ATRG for the square lattice and the simple cubic lattice Ising models. Although the accuracy of the present method degrades than HOTRG with the same bond dimension, the accuracy with fixed computation time is improved greatly from the conventional HOTRG due to the drastic reduction of the computation cost.

Understanding critical phenomena observed universally in many-body systems is one of the central topics in the statistical physics. Due to the difficulties in solving the many-body systems analytically, however, we often have to rely on numerical methods, such as the Monte Carlo method, in the investigation of such complex systems. In recent years, on the other hand, new alternatives, the real-space renormalization group methods, have become popular more and more and many researches have been conducted using these approaches. The *Tensor Renormalization Group* (TRG), proposed by Levin and Nave in 2007, calculates approximately the contraction of tensor network by using the singular value decomposition (SVD) [1]. By representing the partition function of the Ising models by a tensor network, the free energy for the honeycomb or square lattice Ising models is calculated for huge system sizes, which can be regarded virtually as in the thermodynamic limit.

Despite the success of TRG for two-dimensional systems, it is difficult to extend TRG to higher dimensions, because the framework of TRG is tightly related to the two-dimensional lattice topology. In 2012, Xie et al. proposed the *higher-order TRG* (HOTRG) method, which performs the real-space renormalization of tensor networks based on the higher-order singular value decomposition [2]. Unlike TRG, HOTRG can be applied to arbitrary dimensions. Although the computation cost of HOTRG is larger than TRG, its accuracy is higher when we compare these two method with the same bond dimension  $D$ , which is the maximum number of the tensor indices. A lot of methods inspired by TRG and HOTRG have been proposed [3–15], and they have been used for examining classical and quantum systems not only in the condensed matter physics but also in the particle physics [16–30].

Although HOTRG can be applied to higher-dimensional systems in principle, its computation cost in the  $d$ -dimensional lattice model increases quite rapidly as  $O(D^{4d-1})$ , where  $d$  is the dimension of the lattice, as a function of bond dimension  $D$ . Thus, it is totally impractical to apply HOTRG for large bond dimensions and/or high spatial dimensions. New algorithms that can

perform the real-space renormalization in general dimensions with a reasonable cost are strongly demanded.

In this Letter, we propose a new TRG method, referred to as *anisotropic TRG* (ATRG), which drastically reduces the computational complexity for systems on hypercubic lattices by renormalizing tensors in an anisotropic way after tensor decomposition. The computation cost of ATRG scales as  $O(D^{2d+1})$ , which is much lower than that of the conventional HOTRG,  $O(D^{4d-1})$ , while it requires the same memory footprint of  $O(D^{2d})$  as HOTRG. As demonstrations of ATRG, we calculate the free energies of the square lattice and simple cubic lattice Ising models at their critical points, and discuss the advantages of our method over TRG and HOTRG.

Let us begin with describing ATRG algorithm for the two-dimensional square lattice network. Hereafter,  $U_{\{X\}}$ ,  $S_{\{X\}}$ , and  $V_{\{X\}}$  represent respectively the left isometry, the singular value matrix, the right isometry of SVD of matrix  $X$ , *i.e.*,  $X = U_{\{X\}} S_{\{X\}} V_{\{X\}}^t$  or  $X_{ij} = \sum_{\alpha} S_{\{X\}\alpha\alpha} U_{\{X\}i\alpha} V_{\{X\}j\alpha}$ . In ATRG, we renormalize two neighboring tensors in the horizontal ( $x$ ) and the vertical ( $y$ ) directions alternately as in the same way as HOTRG. The outline of ATRG renormalization step along  $y$  direction is shown in FIG. 1.

First, four-leg tensor  $T$  with bond dimension  $D$  is decomposed by SVD, and the bond dimension of the singular value matrix is truncated by  $D$  [step (a) in FIG. 1]:

$$T_{y_0 y_1 x_0 x_1} \approx \sum_{\alpha=1}^D S_{\{T\}\alpha\alpha} U_{\{T\}y_0 x_0 \alpha} V_{\{T\}y_1 x_1 \alpha}. \quad (1)$$

Then, we define four tensors,  $A$ ,  $B$ ,  $C$ ,  $D$ , as

$$A_{y_0 x_0 \alpha} = U_{\{T\}y_0 x_0 \alpha}, \quad (2)$$

$$B_{y_1 x_1 \alpha} = S_{\{T\}\alpha\alpha} V_{\{T\}y_1 x_1 \alpha}, \quad (3)$$

$$C_{y_1 x_2 \beta} = S_{\{T\}\beta\beta} U_{\{T\}y_1 x_2 \beta}, \quad (4)$$

$$D_{y_2 x_3 \beta} = V_{\{T\}y_2 x_3 \beta} \quad (5)$$

[step (a) in FIG. 1]. Note that the accuracy of the final free energy may depend on how to separate the singular value matrix in the above step. Indeed, we observe that

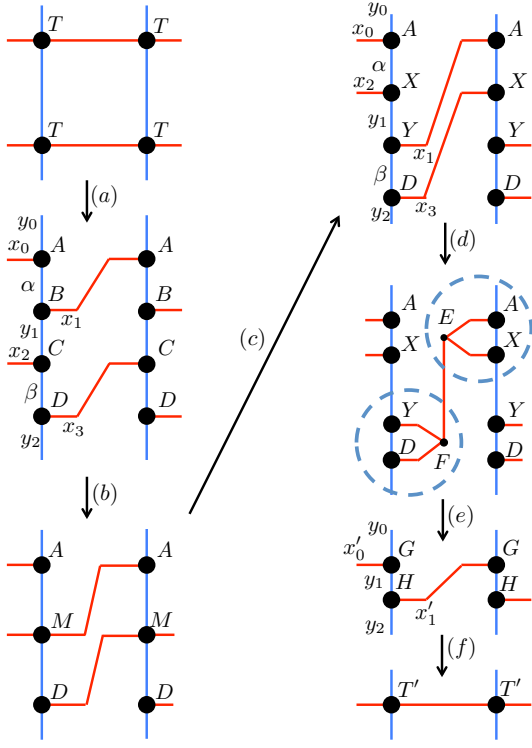


FIG. 1. Renormalization step of ATRG in  $y$  direction for the two-dimensional square lattice model.

by including the singular matrix  $S$  in  $B$  and  $C$ , the error of the final free energy is minimized. Such a construction gives us a better free energy than the equal weight decomposition,  $\sqrt{S}$ , of the singular matrix into  $A$  and  $B$  (or  $C$  and  $D$ ).

Next, by using SVD, we swap the bond of  $B$  and  $C$  [step (b) and (c) in FIG. 1]. In order to swap the  $x_1$  bond of  $B$  and  $x_2$  bond of  $C$ , we define tensor  $M$  as

$$M_{\alpha\beta x_1 x_2} = \sum_{y_1} B_{y_1 x_1 \alpha} C_{y_1 x_2 \beta}, \quad (6)$$

and, by SVD of  $M$  and truncating the singular values to  $D$ , we define new  $X$  and  $Y$  as

$$M_{\alpha\beta x_1 x_2} \approx \sum_{y_1}^D S_{\{M\}y_1 y_1} U_{\{M\}\alpha x_2 y_1} V_{\{M\}\beta x_1 y_1}, \quad (7)$$

$$X_{\alpha x_2 y_1} = \sqrt{S_{\{M\}y_1 y_1}} U_{\{M\}\alpha x_2 y_1}, \quad (8)$$

$$Y_{\beta x_1 y_1} = \sqrt{S_{\{M\}y_1 y_1}} V_{\{M\}\beta x_1 y_1}. \quad (9)$$

Then, we renormalize the horizontal two bonds into one by using projectors  $E$  and  $F$  [step (d) and (e) in FIG. 1]. By applying projector  $E$  ( $F$ ) to  $A$  and  $X$  ( $Y$  and  $D$ ), we obtain new tensor  $G$  ( $H$ ) as

$$G_{y_0 y_1 x'_0} = \sum_{\alpha, x_0, x_2} A_{y_0 x_0 \alpha} X_{\alpha x_2 y_1} E_{x_0 x_2 x'_0}, \quad (10)$$

$$H_{y_1 y_2 x'_1} = \sum_{\beta, x_1, x_3} D_{y_2 x_3 \beta} Y_{\beta x_1 y_1} F_{x_1 x_3 x'_1}. \quad (11)$$

Finally, a new renormalized tensor,  $T'$ , is made from the product of  $G$  and  $H$  as

$$T'_{y_0 y_2 x'_0 x'_1} = \sum_{y_1} G_{y_0 y_1 x'_0} H_{y_1 y_2 x'_1}, \quad (12)$$

[step (f) in FIG. 1], which will be used as an input to the next renormalization step in  $x$  direction.

As for the choice of projectors,  $E$  and  $F$ , there are many possibilities. Here, we perform the projection in the following way:

$$\begin{aligned} Q_{y_0 y_1 y_2 y_3} &= \sum_{x_1 x_3 \alpha \beta} Y_{\beta y_1 x_1} D_{y_2 x_3 \beta} A_{y_0 x_1 \alpha} X_{\alpha x_3 y_3} \\ &\approx \sum_{x'_1}^D S_{\{Q\}x'_1 x'_1} U_{\{Q\}y_1 y_2 x'_1} V_{\{Q\}y_0 y_3 x'_1}, \end{aligned} \quad (13)$$

$$H_{y_1 y_2 x'_1} = \sqrt{S_{\{Q\}x'_1 x'_1}} U_{\{Q\}y_1 y_2 x'_1}, \quad (14)$$

$$G_{y_0 y_3 x'_1} = \sqrt{S_{\{Q\}x'_1 x'_1}} V_{\{Q\}y_0 y_3 x'_1}. \quad (15)$$

Unlike the conventional HOTRG, the projectors are not necessarily isometries. In addition, when we calculate only the free energy,  $G$  and  $H$  can be directly obtained through SVD as Eqs. (13)-(15). The explicit form of the projectors is needed for calculating other physical quantities, *e.g.*, energy and magnetization.

The whole renormalization step described above can be performed with computation cost of  $O(D^5)$  and memory footprint of  $O(D^4)$  by performing the partial SVD using the Arnoldi method or other techniques. The computation cost of ATRG is the same as TRG with partial or randomized SVD [11].

Note that in step (a) of FIG. 1, there is the freedom of choosing the bond used by  $A$  from two bonds in  $x$  direction,  $x_0$  and  $x_1$ . By choosing the pair of bonds used for  $A'$  in the following renormalization step properly, we can skip SVD of  $T'$  by using  $G$  and  $H$ , and continue calculation without additional truncation errors (FIG. 2). If the bond geometry of  $A'$  and  $B'$  (or  $C'$  and  $D'$ ) are chosen so that they match the geometry of  $G$  and  $H$ , respectively, there occur no truncation errors at the decomposition of  $T'$ . Note that explicit SVD of  $T'$  needs computation cost of  $O(D^5)$ . This cost can be reduced to  $O(D^4)$  by performing SVDs of  $G$  and  $H$ , and taking SVD of the intermediate 2-bond tensor,  $K$ , defined as  $K = S_{\{G\}} V_{\{G\}}^t U_{\{H\}} S_{\{H\}}$ .

One of the important differences between ATRG and HOTRG is that in ATRG, before applying the projectors  $E$  and  $F$ , we construct  $X$  and  $Y$  from a low-rank approximation of  $M$ , which is constructed from  $B$  and

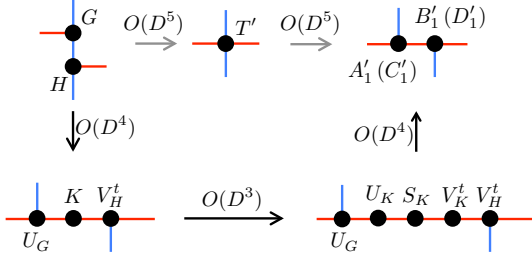


FIG. 2. Reduction of SVD computation cost for the two-dimensional square lattice model. Here,  $K = S_{\{G\}} V_{\{G\}}^t U_{\{H\}} S_{\{H\}}$ .

$C$  [step (b) and (c) in FIG. 1]. In this low-rank approximation, the truncation from  $D^2$  to  $D$  happens, and thus ATRG involves an additional approximation compared with HOTRG.

One can easily generalize ATRG to systems in dimensions higher than two. As an example, we illustrate the renormalization step of ATRG in three dimensions in FIG. 3. For general  $d$ -dimensional hypercubic lattice, ATRG can renormalize tensors with computation cost of  $O(D^{2d+1})$  and memory footprint of  $O(D^{2d})$ .

It is naively expected that we have to perform SVD with  $O(D^{2d+1})$  computation cost both for swapping bonds [step (c)] and making projectors [step (d)]. However, the latter cost can be reduced to  $O(D^{\max(d+3,7)})$  as shown in FIG. 4, where  $A$ ,  $X$ ,  $Y$ , and  $D$  in FIG. 1 are represented as three-bond tensors with bond dimensions  $D^{d-1}, D, D$ . In FIG. 4, before making projectors, SVD or the QR decomposition is performed for each tensor. By introducing this preprocess, the cost of SVDs for making projectors in step (d) and (e) in FIG. 3 is reduced to  $O(D^{\max(d+3,7)})$ , which means the cost of SVDs for making projectors becomes subleading for  $d > 3$ .

We apply ATRG to the two- and three-dimensional Ising models at the critical temperature. All axes are renormalized 15 times alternately, i.e., the system contains  $(2^{15})^d$  spins. First, we discuss the two-dimensional Ising model on a square lattice. The free energy density obtained by ATRG at  $T = T_c = 2/\log(1 + \sqrt{2})$  [31] is shown in FIGs. 5 and 6. In FIG. 5, we plot the absolute error of the free energy density as a function of bond dimension  $D$ . We calculate up to  $D = 108$  ( $D = 58$ ) for TRG and ATRG (HOTRG). For all  $D$ , the result of ATRG is between those of TRG and HOTRG. Note that ATRG has the same computation cost as TRG, while the cost of HOTRG is higher. In order to investigate the performance of ATRG more precisely, we compare the  $D$  dependence of the error with fixed computation time. For that purpose we introduce the leading-order computation time  $\tau$  (dimensionless quantity) defined as

$$\tau = \begin{cases} D^5 & \text{for TRG and ATRG} \\ D^7 & \text{for HOTRG} \end{cases} \quad (16)$$

based on their leading computation cost. In FIG. 6, we

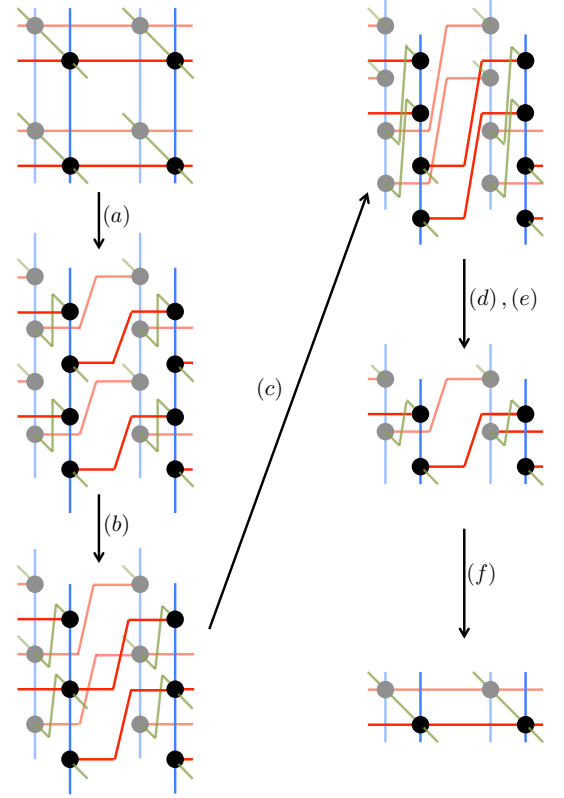


FIG. 3. Renormalization step of ATRG in  $z$  direction for the three-dimensional simple cubic lattice model.

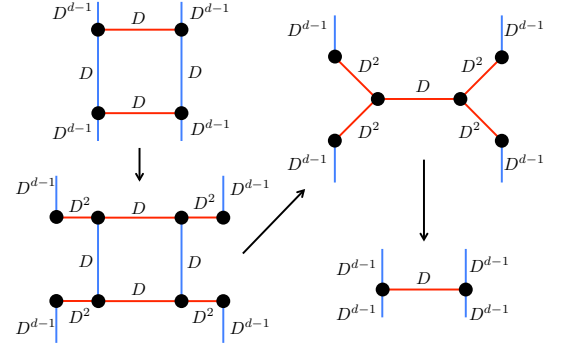


FIG. 4. Reduction of SVD cost in step (d) and (e) in FIG. 3 for  $d > 3$ .

plot the absolute error of the free energy density as a function of  $\tau$  for the three methods. With fixed  $\tau$ , ATRG shows the smallest error among the three methods. Note that the partial SVD is the most expensive operation in ATRG, while it is the contraction in HOTRG. In practice, the partial SVD takes much longer time than the contraction, even when their computation costs are in the same order. Thus, the actual performance difference between ATRG and HOTRG is smaller than FIG. 6, though ATRG becomes more and more advantageous for larger

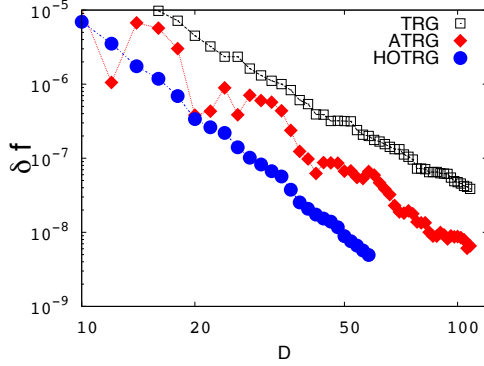


FIG. 5. Absolute error of the free energy density of the two-dimensional Ising model at  $T = T_c$  as a function of bond dimension  $D$  calculated by TRG (black squares), HOTRG (blue circles), and ATRG (red diamonds). Even though ATRG has the same computation cost as TRG, it produces more accurate results than TRG.

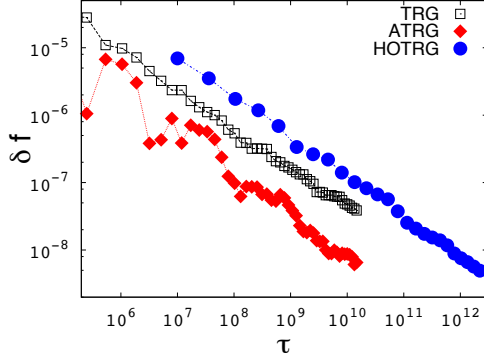


FIG. 6. Absolute error of the free energy density of the two-dimensional Ising model at  $T = T_c$  as a function of leading-order computation time  $\tau$  [Eq. (16)] calculated by TRG (black squares), HOTRG (blue circles), and ATRG (red diamonds). ATRG achieves the most accurate results among the three methods with fixed computation time.

$D$  due to the difference in order in computational cost [Eq. (16)].

It should be mentioned that the present method suffered from larger and nonmonotonic fluctuations in the convergence of the error. This observed behavior is probably related to the two independent truncations in the ATRG renormalization procedure. Because ATRG optimizes only the local tensors in each truncation, increasing  $D$  does not necessarily improve the accuracy of the free energy, which is determined by the global tensor network. The nonmonotonic convergence in ATRG should be subjected to further investigation.

Next, we move to the three-dimensional Ising model on a simple cubic lattice. In the three-dimensional case,

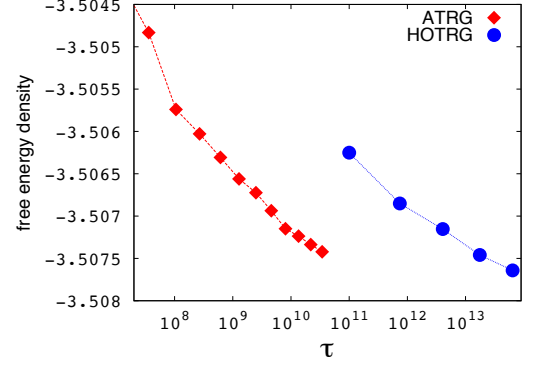


FIG. 7. Free energy density of the three-dimensional Ising model at  $T = T_c$  as a function of leading-order computation time  $\tau$  [Eq. (17)] calculated by HOTRG (blue circles) and ATRG (red diamonds). ATRG achieves much lower free energy than HOTRG with fixed computation time.

we compare ATRG with HOTRG. In FIG. 7, we show the free energy density as a function of  $\tau$  at  $T = T_c = 4.5115$  [2, 32–34]. Here, we again define the leading-order computation time  $\tau$  for three dimensions as

$$\tau = \begin{cases} D^7 & \text{for ATRG} \\ D^{11} & \text{for HOTRG.} \end{cases} \quad (17)$$

In the present case, we calculate up to  $D = 32$  ( $D = 18$ ) for ATRG (HOTRG). In FIG. 7, it is clearly demonstrated again that the ATRG gives the better (lower) free energy density than that of HOTRG for the same leading-order computation time  $\tau$ . We expect that the advantage of ATRG over HOTRG should be more pronounced in higher dimensions.

In summary, we proposed the ATRG method that can perform tensor renormalization operations with computation cost of  $O(D^{2d+1})$  and memory footprint of  $O(D^{2d})$  in  $d$  dimensions. The computational cost of the proposed method is much lower than that of the conventional HOTRG,  $O(D^{4d-1})$ , which enables us to apply the tensor renormalization method in higher dimensions. Unlike HOTRG, our algorithm involves the truncation of the bond dimension by using SVD when we swap the bonds of two tensors [step (b) and (c) in FIG. 1]. Due to the additional approximation, the accuracy in the final result degrades compared with HOTRG. However, this disadvantage is compensated by the drastic reduction of the computational cost from  $O(D^{4d-1})$  to  $O(D^{2d+1})$ . We confirmed that for two- and three-dimensional Ising models our method achieve higher accuracy than HOTRG with fixed leading-order computational time. Since ATRG is a real space renormalization method similar to HOTRG, and preserves the lattice topology after the renormalization, it can be applied to various lattice systems in arbitrary dimensions

Finally, as we pointed out already, the partial SVD is the most expensive operation in ATRG. The performance of the partial SVD is thus essential in ATRG, and development of more efficient and stable partial SVD algorithms is desired for future application of ATRG to large-scale complex lattice systems.

The authors would like to thank Takuya Yamamoto

and Hayate Nakano for careful reading of the manuscript and comments. D. A. is supported by the Japan Society for the Promotion of Science through the Program for Leading Graduate Schools (MERIT). This work is partially supported by MEXT as Exploratory Challenge on Post-K computer (Frontiers of Basic Science: Challenging the Limits) and by JSPS KAKENHI No. 15K17701, 17K05564, and 19K03740.

- 
- [1] M. Levin and C. P. Nave, Phys. Rev. Lett. **99**, 120601 (2007).
  - [2] Z. Y. Xie, J. Chen, M. P. Qin, J. W. Zhu, L. P. Yang, and T. Xiang, Phys. Rev. B **86**, 045139 (2012).
  - [3] Z.-C. Gu and X.-G. Wen, Phys. Rev. B **80**, 155131 (2009).
  - [4] Z. Y. Xie, H. C. Jiang, Q. N. Chen, Z. Y. Weng, and T. Xiang, Phys. Rev. Lett. **103**, 160601 (2009).
  - [5] G. Evenbly and G. Vidal, Phys. Rev. Lett. **115**, 180405 (2015).
  - [6] G. Evenbly, Phys. Rev. B **95**, 045117 (2017).
  - [7] M. Bal, M. Mariën, J. Haegeman, and F. Verstraete, Phys. Rev. Lett. **118**, 250602 (2017).
  - [8] S. Yang, Z.-C. Gu, and X.-G. Wen, Phys. Rev. Lett. **118**, 110504 (2017).
  - [9] M. Hauru, C. Delcamp, and S. Mizera, Phys. Rev. B **97**, 045111 (2018).
  - [10] K. Harada, Phys. Rev. B **97**, 045124 (2018).
  - [11] S. Morita, R. Igarashi, H.-H. Zhao, and N. Kawashima, Phys. Rev. E **97**, 033310 (2018).
  - [12] C. Wang, S.-M. Qin, and H.-J. Zhou, Phys. Rev. B **90**, 174201 (2014).
  - [13] H.-H. Zhao, Z.-Y. Xie, T. Xiang, and M. Imada, Phys. Rev. B **93**, 125115 (2016).
  - [14] G. Evenbly, Phys. Rev. B **98**, 085155 (2018).
  - [15] A. J. Ferris, Phys. Rev. B **87**, 125139 (2013).
  - [16] W. Li, S.-S. Gong, Y. Zhao, S.-J. Ran, S. Gao, and G. Su, Phys. Rev. B **82**, 134434 (2010).
  - [17] H. H. Zhao, Z. Y. Xie, Q. N. Chen, Z. C. Wei, J. W. Cai, and T. Xiang, Phys. Rev. B **81**, 174411 (2010).
  - [18] Q. N. Chen, M. P. Qin, J. Chen, Z. C. Wei, H. H. Zhao, B. Normand, and T. Xiang, Phys. Rev. Lett. **107**, 165701 (2011).
  - [19] B. Ditttrich and F. C. Eckert, J. Phys.: Conf. Ser. **360**, 012004 (2012).
  - [20] H. C. Jiang, Z. Y. Weng, and T. Xiang, Phys. Rev. Lett. **101**, 090603 (2008).
  - [21] G. Evenbly and G. Vidal, Phys. Rev. Lett. **116**, 040401 (2016).
  - [22] Y. Meurice, Phys. Rev. B **87**, 064422 (2013).
  - [23] S. Wang, Z.-Y. Xie, J. Chen, N. Bruce, and T. Xiang, Chin. Phys. Lett. **31**, 070503 (2014).
  - [24] J. F. Yu, Z. Y. Xie, Y. Meurice, Y. Liu, A. Denblyker, H. Zou, M. P. Qin, J. Chen, and T. Xiang, Phys. Rev. E **89**, 013308 (2014).
  - [25] H. Ueda, K. Okunishi, and T. Nishino, Phys. Rev. B **89**, 075116 (2014).
  - [26] J. Genzor, A. Gendiar, and T. Nishino, Phys. Rev. E **93**, 012141 (2016).
  - [27] L.-P. Yang, Y. Liu, H. Zou, Z. Y. Xie, and Y. Meurice, Phys. Rev. E **93**, 012138 (2016).
  - [28] H. Kawauchi and S. Takeda, Phys. Rev. D **93**, 114503 (2016).
  - [29] R. Sakai, S. Takeda, and Y. Yoshimura, Prog. Theor. Exp. Phys. **2017**, 063B07 (2017).
  - [30] Y. Yoshimura, Y. Kuramashi, Y. Nakamura, S. Takeda, and R. Sakai, Phys. Rev. D **97**, 054511 (2018).
  - [31] L. Onsager, Phys. Rev. **65**, 117 (1944).
  - [32] Y. Deng and H. W. J. Blöte, Phys. Rev. E **68**, 036125 (2003).
  - [33] M. Hasenbusch, Phys. Rev. B **82**, 174433 (2010).
  - [34] J. Kaupužs, R. V. N. Melnik, and J. Rimšāns, Int. J. Mod. Phys. C **28**, 1750044 (2017).